[2-^{11}C]Isopropyl-, [1-^{11}C]Ethyl-, and [^{11}C]Methyl-Labeled Phenoxyphenyl Acetamide Derivatives as Positron Emission Tomography Ligands for the Peripheral Benzodiazepine Receptor: Radiosynthesis, Uptake, and in Vivo Binding in Brain

Ming-Rong Zhang,*[,†,‡] Masanao Ogawa,[†,‡] Jun Maeda,[§] Takehito Ito,[†,‡] Junko Noguchi,[‡,§] Katsushi Kumata,[†,||] Takashi Okauchi,[§] Tetsuya Suhara,[§] and Kazutoshi Suzuki[†]

Department of Medical Imaging, National Institute of Radiological Sciences, 4−9−1 Anagawa, Inage-ku, Chiba 263-8555, Japan, Brain Imaging Project, National Institute of Radiological Sciences, 4−9−1 Anagawa, Inage-ku, Chiba 263-8555, Japan, SHI Accelerator Service Co. Ltd., 5−9−11 Kitashinagawa, Shinagawa-ku, Tokyo 141-8686, Japan, and WDB Co. Ltd., 2−6−2 Ohte, Chiyoda-ku, Tokyo 100-0004, Japan

Received January 4, 2006

The peripheral benzodiazepine receptor (PBR) is widely expressed in peripheral tissues, blood cells, and in glia cells in the brain. We have previously developed two positron emission tomography (PET) ligands, *N*-(2-[^{11}C],5-dimethoxybenzyl)-*N*-(5-fluoro-2-phenoxyphenyl)acetamide ([^{11}C]**2**) and its [^{18}F]fluoroethyl analogue ([^{18}F]**6**), for the current investigation of PBR in the human brain. The aim of this study was to label the potent PBR agonist *N*-(4-chloro-2-phenoxyphenyl)-*N*-(isopropoxybenzyl)acetamide (**3**) and its ethyl (**7**) and methyl (**8**) homologues with ^{11}C and to evaluate them as PET ligands for PBR with mice, rats, and monkeys. Ligands [^{11}C]**3**, [^{11}C]**7**, and [^{11}C]**8** were synthesized by alkylation of phenol precursor **9** with 2-[2-^{11}C]iodopropane ([^{11}C]**10**), [1-^{11}C]iodoethane ([^{11}C]**11**), and [^{11}C]iodomethane ([^{11}C]**12**), respectively. The alkylating agent [^{11}C]**10** or [^{11}C]**11** was prepared by reacting CH_3MgBr with [^{11}C]CO_2, followed by reduction with $LiAlH_4$ and iodination with HI. In vitro quantitative autoradiography determined that **3**, **7**, and **8** had potent binding affinities (K_i = 0.07−0.19 nM) for PBR in the rat brain. These [^{11}C]ligands could pass across the blood−brain barrier and enter the rat brain (0.17−0.32% of injected dose per gram wet tissue). Ex vivo autoradiography showed that the [^{11}C]ligands preferably distributed in the olfactory bulb and cerebellum, two regions with richer PBR density in the rat brain. The co-injection of PBR-selective **2** reduced the [^{11}C]ligand binding in the two regions, suggesting that binding in the rat brain was specific to PBR. PET study determined that the [^{11}C]ligands preferably accumulate in the occipital cortex of the monkey brain, a region with a high density of PBR in the primate brain. Moreover, in vivo binding of the methyl homologue [^{11}C]**8** in the monkey brain could be inhibited by PBR-selective **2** or **1**, indicating that some of the [^{11}C]**8** binding was due to PBR. Metabolite analysis demonstrated that these [^{11}C]ligands were metabolized by debenzylation to polar products mainly in the plasma.

Introduction

The peripheral benzodiazepine receptor (PBR) is a protein in which the critical component (18-kDa protein) of a multimeric 140−200-kDa complex[1] locates in the outer mitochondrial membrane[2] and enriches in the outer/inner mitochondrial membrane contact sites at the cellular level.[3] PBR is widely expressed in the peripheral organs, including the kidney, nasal epithelium, lung, heart, and endocrine organs, such as the adrenal, testis, and pituitary gland.[4−7] In the central nervous system, PBR is mainly distributed in the olfactory bulb and cerebellum of mice and rats and in the occipital cortex of primates.[8−12] Clinical investigations for PBR revealed that this protein is relative to various human pathologies, including ischemia−reperfusion injury,[13] neurodegenerative diseases,[14] brain damage,[15] psychiatric disorders,[16] and cancer.[17] These findings have prompted the development of a positron emitter tomography (PET) ligand for PBR that can be used to image this protein and to measure its level in vivo in both humans and animals.[18−22]

(*R*)-(1-(2-Chlorophenyl)-*N*-[^{11}C]methyl-*N*-(1-methylpropyl)-isoquinoline ([^{11}C]-(*R*)-PK11195, [^{11}C]**1**, Scheme 1) is the first PET ligand for diagnostic imaging in patients suffering from glioblastoma multiforme.[23] However, PBR imaging in primate brain with [^{11}C]**1** was sometimes unsuccessful, since its uptake into the brain was not high enough for quantitative analysis.[24] In 1998, novel phenoxyphenyl acetamide derivates were reported with potent and selective binding affinities for PBR.[25] Among these compounds, two promising ligands, *N*-(2,5-dimethoxybenzyl)-*N*-(5-fluoro-2-phenoxyphenyl)acetamide (DAA1106, **2**, Scheme 1) and *N*-(4-chloro-2-phenoxyphenyl)-*N*-(isopropoxybenzyl)acetamide (DAA1197, **3**), were identified for their pharmacological properties relative to PBR.[26−28] The two compounds displayed higher affinities for PBR in the mitochondrial fractions of animal brains than **1** and weak or negligible affinities for receptors, ion channels, uptake/transporters, and second messengers.[26,27] However, despite their high affinity for PBR and similar structures, the two compounds differed in their respective interactions with PBR.[28] It was assayed that **3** is a putative PBR agonist activating the steroid synthesis, while **2** has an antagonistic property for PBR.[28]

To develop a PET ligand for imaging PBR in the brain, we established compounds **2** and **3** as our research targets with the expectation that they would display improved or different properties from [^{11}C]**1**. We first labeled antagonist **2** with ^{11}C and then synthesized three novel [^{18}F]fluoroalkyl analogues

* Corresponding author. Tel: 81-43-206-4041. Fax: 81-43-206-3261. E-mail: zhang@nirs.go.jp.
† Department of Medical Imaging, National Institute of Radiological Sciences.
‡ SHI Accelerator Service Co. Ltd.
§ Brain Imaging Project, National Institute of Radiological Sciences.
|| WDB Co. Ltd.

10.1021/jm060006k CCC: $33.50
Published on Web 04/12/2006

Scheme 1. Chemical Structures of [^{11}C]1 ([^{11}C](*R*)-PK11195), [^{11}C]2 ([^{11}C]DAA1106), and [^{11}C]3 ([^{11}C]DAA1097) Analogues

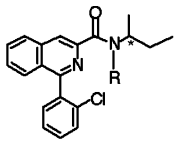

(*R*)-PK11195 (**1**): R = CH_3
[^{11}C](*R*)-PK11195 ([^{11}C]**1**): R = $^{11}CH_3$

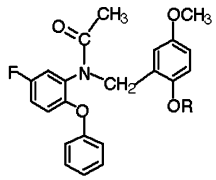

DAA1106 (**2**): R = CH_3
[^{11}C]DAA1106 ([^{11}C]**2**): R = $^{11}CH_3$
[^{18}F]**4**: R = $^{18}FCH_2$
[^{18}F]**5**: R = $^{18}FCD_2$
[^{18}F]FEDAA1106 ([^{18}F]**6**): R = $^{18}FCH_2CH_2$

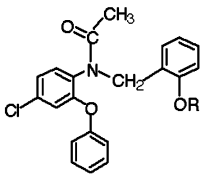

DAA1097 (**3**): R = $CH(CH_3)_2$
[^{11}C]**3**: R = $^{11}CH(CH_3)_2$
7: R = CH_2CH_3
[^{11}C]**7**: R = $^{11}CH_2CH_3$
8: R = CH_3
[^{11}C]**8**: R = $^{11}CH_3$

([^{18}F]**4**−**6**) (Scheme 1).[29−33] The in vitro and in vivo evaluation demonstrated that [^{11}C]**2** and [^{18}F]**6** had higher binding affinities for PBR, higher uptakes, and better in vivo specific binding in the brains than [^{11}C]**1**. [^{11}C]**2** and [^{18}F]**6** are currently being used for the clinical investigation of PBR in human brains in our laboratory.

Here, we continued to label agonist **3** with ^{11}C to provide an alternative PET ligand with a different property from [^{11}C]**2**. Using **3** as the lead ligand, we further labeled its ethyl (**7**) and methyl (**8**) homologues with ^{11}C to probe the in vivo structure−activity relationship of this series of derivatives. Using an autoradiography technique, we measured the in vitro binding affinities (K_i) of **3**, **7**, and **8** to PBR and examined their in vivo specific binding to PBR in rat brain. Using PET, we determined the uptakes of the [^{11}C]ligands and further elucidated the specific binding of the methyl homologue [^{11}C]**8** to PBR in the monkey brain. Finally, we assayed the percentages of the unmetabolized [^{11}C]ligands in mouse plasma and brain and in monkey plasma.

Results and Discussion

Radiosynthesis. The nonradioactive ethyl (**7**) and methyl (**8**) homologues were prepared according to the reaction sequences delineated in Scheme 2. The reaction of phenol precursor **9**[25] with iodoethane (**11**) and iodomethane (**12**) in the presence of NaH afforded **7** and **8** in high chemical yields.

[^{11}C]**3**, [^{11}C]**7**, and [^{11}C]**8** were synthesized by reacting **9** with 2-[2-^{11}C]iodopropane ([^{11}C]**10**), [1-^{11}C]iodoethane ([^{11}C]**11**), and [^{11}C]iodomethane ([^{11}C]**12**), respectively (Scheme 2). Until now, there has been no report about the efficient synthesis of [^{11}C]-**10** with a high specific activity and reproducible radiochemical yield. [^{11}C]**10** has only been reported as a low-yield byproduct in the preparation of [^{11}C]**11** using the Grignard reaction.[34−36] As shown in Scheme 2, the Grignard reagent CH_3MgBr reacted with [^{11}C]CO_2 to yield [1-^{11}C]$CH_3COOMgBr$, which further reacted with excess CH_3MgBr to yield [2-^{11}C]$(CH_3)_2C(OMgBr)_2$. This intermediate was then reduced and iodinated to form [^{11}C]**10** mixed with [^{11}C]**11**, which was produced simultaneously with a low ratio.

Here, we tried to achieve the selective and efficient synthesis of [^{11}C]**10** or [^{11}C]**11** by promoting or controlling the reaction of two molecules of CH_3MgBr with [^{11}C]CO_2. Moreover, to guarantee a reproducible radiochemical yield and a high specific activity of [^{11}C]**10** or [^{11}C]**11**, we constructed an automated synthesis system using a loop method in place of the conventional one-pot method.[36] This system included the following sequences: (1) trapping [^{11}C]CO_2 produced by the cyclotron into a coil, (2) transferring [^{11}C]CO_2 into a loop loaded with CH_3MgBr to perform the Grignard reaction, (3) producing [^{11}C]-alkyl iodide by reduction and iodination in a reactor vessel, (4) purifying them by gas chromatography.[37] After CH_3MgBr/THF solution was loaded into a polypropylene loop, the target-produced [^{11}C]CO_2 was transferred into this loop to perform the Grignard reaction, followed by reduction with $LiAlH_4$ and iodination with HI. When the reaction mixture of CH_3MgBr and [^{11}C]CO_2 in the loop was kept at 25 °C for 5.0 min, [^{11}C]-**10** yielded a ratio of 80% in the product, while [^{11}C]**11** yielded a ratio of 10%. When the reaction mixture in the loop was cooled at −5 °C for 1.5 min, [^{11}C]**10** was preferably yielded with a ratio of 91% in the product. [^{11}C]**10** and [^{11}C]**11** were purified by gas chromatography with radiochemical purities of >95%. On the other hand, [^{11}C]**12** was produced by reducing [^{11}C]CO_2 with $LiAlH_4$ and iodination with HI (Scheme 2).[38]

Scheme 2. Chemical Synthesis and Radiosynthesis[a]

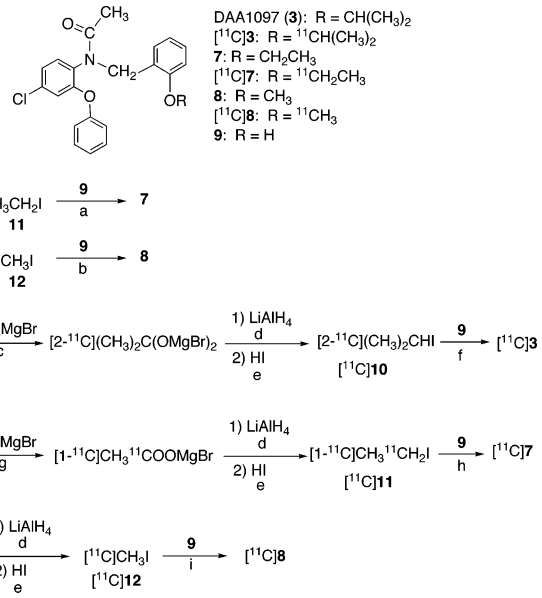

[a] (a) NaH, DMF, 25 °C, 5 h; (b) NaH, DMF, 25 °C, 3 h; (c) 25 °C , 5 min; (d) THF, 180 °C , 1 min; (e) 180 °C , 3 min; (f) NaH, DMF, 130 °C, 10 min; (g) −5 °C, 1.5 min; (h) NaH, DMF, 50 °C, 5 min; (i) NaH, DMF, 30 °C, 5 min.

Alkylations of phenol precursor **9** with [^{11}C]**10**, [^{11}C]**11**, and [^{11}C]**12** were achieved in the presence of NaH under different temperatures, respectively. The reaction efficiency using isopropyl [^{11}C]**10** was 15−25%, while that using ethyl [^{11}C]**11** and methyl [^{11}C]**12** was high (60−80%), suggesting that the alkylation proceeded via an S_N2 mechanism. After the alkylations, HPLC purifications of the reaction mixtures gave [^{11}C]**3**, [^{11}C]**7**, and [^{11}C]**8** in 5 ± 3% (n = 3), 12 ± 9% (n = 3), and 39 ± 10% (n = 3) radiochemical yields based on [^{11}C]CO_2 corrected for the decay. Their synthesis times were 47 ± 4 min for [^{11}C]**3**, 38 ± 3 min [^{11}C]**7**, and 20 ± 1 min for [^{11}C]**8** from the end of bombardment. The identities of these products were confirmed by co-injection with the corresponding nonradioactive **3**, **7**, and **8** on analytic HPLC, respectively. In the final product solutions, the radiochemical purities of [^{11}C]**3**, [^{11}C]**7**, and [^{11}C]-**8** were higher than 98%. Their specific activities were 25−41 GBq/μmol for [^{11}C]**7** and [^{11}C]**8**, while that was 110−145 GBq/μmol for [^{11}C]**3** determined by comparison of the assayed

Table 1. In Vitro Binding Affinity (K_i) for the Peripheral Benzodiazepine Receptor (PBR) and the Central Benzodiazepine Receptor (CBR), and Octanol/Phosphate Buffer Distribution Coefficient (log *D*)

		K_i (nM)[a]			
		PBR			
ligand	R	for [^{11}C]**1**[b]	for [^{11}C]**2**[b]	CBR[c]	log *D*[d]
3 (DAA1097)	$(CH_3)_2CH$	0.19 ± 0.02	0.68 ± 0.02	>1000	4.02
7	CH_3CH_2	0.098 ± 0.01	0.41 ± 0.01	>1000	3.81
8	CH_3	0.074 ± 0.08	0.31 ± 0.68	>1000	3.74
2 (DAA1106)		0.095 ± 0.02	0.16 ± 0.02	>1000	3.65
1 (PK11195)		0.54 ± 0.24	0.82 ± 0.24	>1000	2.78

[a] Values represent the mean obtained from nine concentrations of compound using at least eight slices of rat brain ($n = 3$). [b] [^{11}C]**1** and [^{11}C]**2** were incubated in the presence of the compounds examined, respectively. [c] [^{11}C]Flumazenil was incubated in the presence of the compounds examined. [d] The log *D* values were determined in the phosphate buffer (pH = 7.4)/octanol system using the shaking flask method. All results are presented as mean values ($n = 3$) with a maximum range of ±5%.

radioactivity to the mass measured from the carrier UV peak on HPLC. No significant UV peaks corresponding to **9** and other chemical impurities were observed in the HPLC charts for these products. The formulated products displayed no radiolysis at 25 °C for at least 180 min after radiosynthesis and were stable as PET ligands while performing evaluation on animals.

In Vitro Binding Assays. The in vitro binding affinities (K_i) of **3**, **7**, and **8** for PBR were determined from competition against the [^{11}C]**1** and [^{11}C]**2** binding to PBR by using quantitative autoradiography[32,33] on rat brain sections. As shown in Table 1, the three homologues displayed potent affinities for PBR (K_i = 0.19−0.074 nM for [^{11}C]**1** and 0.68−0.31 nM for [^{11}C]**2**). Their ranking order was **8** (methyl) >**7** (ethyl) >**3** (isopropyl), suggesting that the steric bulk of these substitution groups is not favorable for expressing the binding affinity, despite the molecular similarity and bioisoteric property of these groups. The methyl homologue **8** displayed 2- or 10-fold higher affinity than **2** or **1**. Considering that these derivatives evolved from the classical benzodiazepine structure, the in vitro binding affinities of **3**, **7**, and **8** for the central benzodiazepine receptor (CBR) were measured by competition against the CBR-selective [^{11}C]flumazenil binding. As shown in Table 1, these homologues did not display significant inhibitory effects ($K_i > 1$ μM) on the [^{11}C]flumazenil binding in the rat brain. The high selectivity of **3**, **7**, and **8** for PBR may be due to their drastic structural difference from the classical benzodiazepine.

Ex Vivo Autoradiography. Thirty minutes after intravenous (iv) injection of [^{11}C]**3**, [^{11}C]**7**, and [^{11}C]**8**, relatively high radioactivity (0.17 ± 0.03%, 0.27 ± 0.05% and 0.32 ± 0.04% of injected dose per gram of wet tissue, $n = 3$/[^{11}C]ligand) was detected in the rat brains, respectively. The findings suggested that these ligands do pass across the brain−blood barrier (BBB), which is a prerequisite for a promising PET ligand for brain imaging.

Figure 1 shows ex vivo autoradiograms of [^{11}C]**3**, [^{11}C]**7**, and [^{11}C]**8** in rat brain. Among the regions examined, the highest radioactivity was observed in the olfactory bulb, having the richest PBR density in the rat brain (upper images, a−c). Following the olfactory bulb, relatively higher radioactivity levels were also detected in the cerebellum, whereas moderate or low uptake was seen in other regions such as the frontal cortex, striatum, and hippocampus. Their distribution patterns were consistent not only with the [^{11}C]**2** and [^{3}H]**1** binding sites in the rat brain[10,29,30] but also with the regional distribution of PBR in mouse and rat brains.[5,9,12]

Then, the in vivo specificities of [^{11}C]**3**, [^{11}C]**7**, and [^{11}C]**8** to PBR were tested by co-injecting nonradioactive **2** at a dose of 1 mg/kg, respectively. As shown in Figure 1 (lower images, d−f), the PBR-selective **2** significantly reduced radioactivity in the brain regions compared with the control group (upper images). The most evident decreases were found in the olfactory bulb (43% for [^{11}C]**3**, 33% for [^{11}C]**7**, 37% for [^{11}C]**8**) and cerebellum (44−58% for the controls). Other brain regions (striatum, frontal cortex, etc.) showed a moderate or low decrease in the percent uptake (63−85%) of [^{11}C]**3**, [^{11}C]**7**, and [^{11}C]**8**. These results revealed high specific bindings of the [^{11}C]-ligands to PBR in the olfactory bulb and cerebellum in the rat brain. On the other hand, using the frontal cortex as a reference region with low PBR density,[26] the ratios of olfactory bulb to frontal cortex were 1.5 for [^{11}C]**3**, 1.5 for [^{11}C]**7**, and 2.3 for [^{11}C]**8**, whereas those of other brain regions to the cortex were about 1. This result supported the specific bindings of the [^{11}C]-ligands to PBR mainly in the olfactory bulb. Among these [^{11}C]-ligands, [^{11}C]**8** appeared to have the highest specific binding in the brain regions, in accord with the rank order of their binding affinities.

Monkey PET. The uptake of [^{11}C]**3**, [^{11}C]**7**, and [^{11}C]**8** in the monkey brains was examined using PET. As the previous in vitro study demonstrated a high density of PBR in the occipital cortex of the postmortem human,[12] we placed the region of interest (ROI) on the occipital cortex in PET experiments. Figure 2 shows typical PET summation images of the monkey brain acquired from 20 to 90 min after the [^{11}C]-ligands injection (70−80 MBq). In these PET images, the higher radioactivity levels present in the occipital cortex in the monkey brain provided visual evidence that [^{11}C]**3**, [^{11}C]**7**, and [^{11}C]**8** are specific ligands for PBR in monkey brains.

Figure 3 shows the time−activity curves (TAC) of [^{11}C]**3** (closed circles), [^{11}C]**7** (squares), and [^{11}C]**8** (open circles) in the occipital cortex. At 2 min after injection, high radioactivity was observed in the occipital cortex, which then remained at almost steady levels until the end of the PET measurement (90 min). The ethyl [^{11}C]**7** and methyl [^{11}C]**8** displayed similar uptake in the occipital cortex. These values were similar to that of [^{11}C]**2** and 4 times higher than that of [^{11}C]**1**, the standard PET ligand for PBR.[30] Compared to the two other ligands, the isopropyl [^{11}C]**3** displayed a slightly lower radioactivity in the corresponding region. The difference between [^{11}C]**7** or [^{11}C]**8** and [^{11}C]**3** may be due to the difference in their binding affinity (**8** > **7** > **3**) and lipophilicity (**3** > **7** > **8**), as shown in Table 1. Since the PBR density is lower in the brain than that in the peripheral organs, the lower affinity of [^{11}C]**3** could reduce its uptake into the brain.

Considering the lipophilicity, simplicity of radiosynthesis, in vitro affinity, uptake, and specific binding, we selected [^{11}C]**8** from the three [^{11}C]ligands for the inhibition experiment. Figure 4 shows the TACs of [^{11}C]**8** in the occipital cortex after treatment with the PBR selective **2** or **1**. Pretreatment with **2** (1.0 mg/kg) reduced the uptake for the TAC (open circles) of [^{11}C]**8** as compared to the control experiment (closed circles) preformed under the same conditions. As shown in Figure 4, the pretreatment enhanced the initial maximal uptake of [^{11}C]-**8**, which might be derived from [^{11}C]**8** being dispossessed by the nonradioactive **2** mass from the lung, which is abundant in PBR. A similar tendency has been reported in the PET studies using [^{11}C]**2**[30] and [^{18}F]**6**.[32] In the [^{3}H]**1** experiment, the radioactivity in the lung was significantly decreased by the co-injection of the nonradioactive **1** at 1 min after injection, whereas the radioactivity in the brain was increased by **1** at 1 min but obviously decreased from 10 min.[39] Until the end of the PET

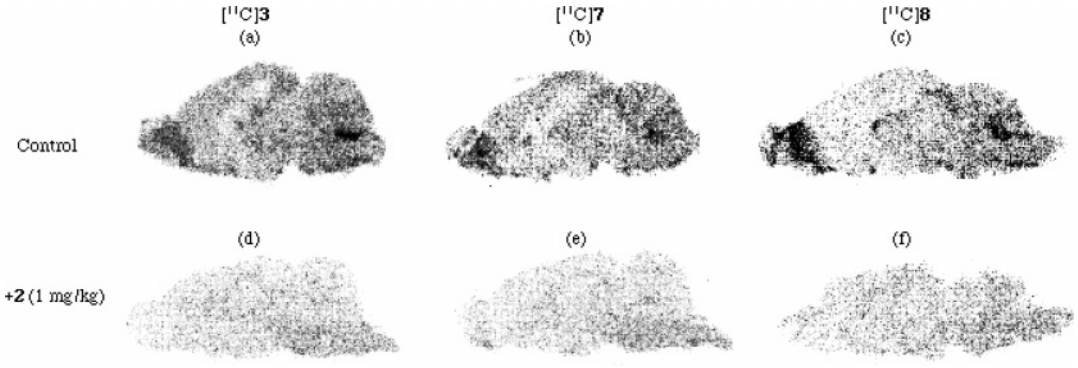

Figure 1. Ex vivo autoradiograms of [^{11}C]**3**, [^{11}C]**7**, and [^{11}C]**8** in the sagittal sections of rat brains at 30 min after injection (45−50 MBq): (a) [^{11}C]**3**, (b) [^{11}C]**7**, (c) [^{11}C]**8**, (d) [^{11}C]**3** + **2** (1 mg/kg), (e) [^{11}C]**7** + **2** (1 mg/kg), (f) [^{11}C]**8** + **2** (1 mg/kg).

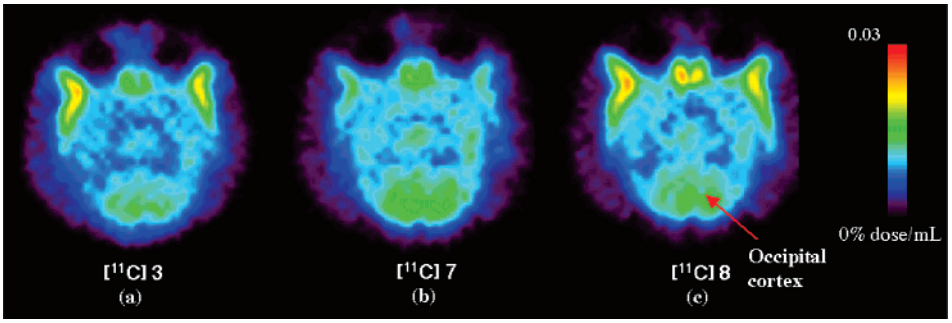

Figure 2. PET summation images of monkey brains acquired between 20 and 90 min after [^{11}C]ligand injection (70−80 MBq). These images were obtained from the same subject: (a) [^{11}C]**3**, (b) [^{11}C]**7**, and (c) [^{11}C]**8**. Relatively high radioactivity was observed in the occipital cortex.

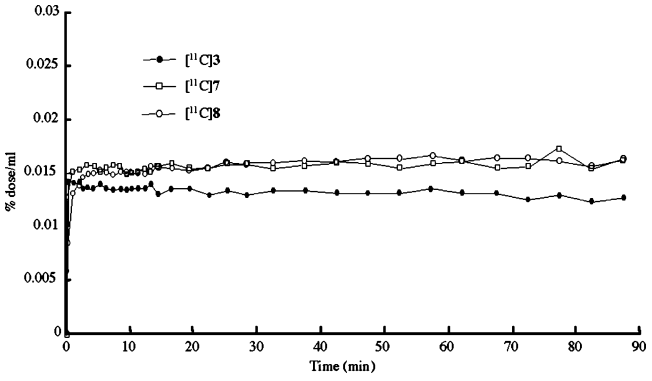

Figure 3. Time−activity curves of [^{11}C]**3** (closed circles), [^{11}C]**7** (squares), and [^{11}C]**8** (open circles) in the occipital cortex of monkey brain after injection between 0 and 90 min. Data were normalized to the percent of injected dose (% dose) per volume (mL).

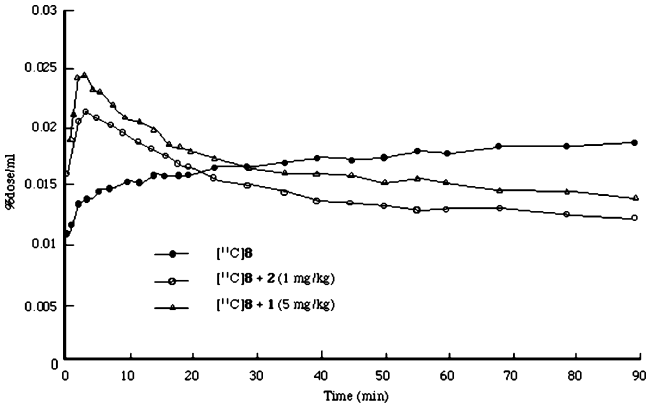

Figure 4. Time−activity curves of [^{11}C]**8** in the occipital cortex of monkey brain after injection between 0 and 90 min. The radioactivity of the control (closed circles) was inhibited by pretreatment with **2** (open circles) or **1** (triangles). Data were normalized to the percent of injected dose (% dose) per volume (mL).

scan, the radioactivity level was reduced to about 60% of the control, suggesting some specific binding of [^{11}C]**8** present in the occipital cortex. Pretreatment with **1** (5 mg/kg) also reduced radioactivity in the occipital cortex to about 70% of the control, as shown in the TAC (triangles). The reduction percentage on the uptake of [^{11}C]**8** by **1** was slightly lower than that by **2**, probably due to the weaker affinity of **1** for PBR and its lower penetration[28] into the brain than that of **2**. Considering that treatment with **1** and **2** increased initial uptakes of [^{11}C]**8**, these TACs could be normalized to the initial maximum uptake of [^{11}C]**8** as 100%. The normalized TACs showed that the uptakes of [^{11}C]**8** were inhibited by **1** and **2** to <50% of the control level by the end of the PET scan. This finding confirmed that [^{11}C]**8** has some specific binding with PBR in the monkey brain, although the binding level was lower than those of [^{11}C]**2**[30] and [^{18}F]**6**.[32]

Metabolite Analysis. In the imaging study, the presence of significant quantities of radioactive metabolites in the target subject may present an insurmountable barrier to the proper quantification of images and interpretation of the results. We therefore performed the metabolite analyses of [^{11}C]**3**, [^{11}C]**7**, and [^{11}C]**8** in mouse plasma and brain and in monkey plasma.

Figure 5 shows the percentages of the unchanged [^{11}C]ligands in the plasma and brain homogenate of mice measured by HPLC. At 5 min after injection, fractions corresponding to the unmetabolized [^{11}C]ligands in the plasma rapidly decreased to 65% for [^{11}C]**8**, 60% for [^{11}C]**7**, and 48% for [^{11}C]**3**, respectively. From 15 min, the [^{11}C]ligands were continuously metabolized in slow rates and remained at a 30−40% level until the end of this experiment. In addition to the parent [^{11}C]ligands, three fractions representing the corresponding [^{11}C]metabolites were observed in the HPLC charts, respectively. As estimated from their retention times (t_R = 1.9−2.7 min), these [^{11}C]-metabolites were much more polar than the parent [^{11}C]ligands (t_R > 8 min). Despite their remarkable metabolism in the plasma,

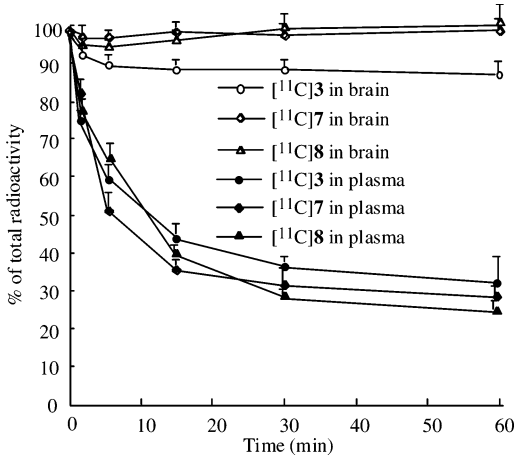

Figure 5. Percent conversion of [^{11}C]**3**, [^{11}C]**7**, or [^{11}C]**8** to [^{11}C]-metabolite in the mouse plasma and brain at several time points after iv injection of [^{11}C]ligand (30−40 MBq) into the mice ($n = 3$).

Scheme 3. In Vivo Metabolic Route of [^{11}C]3, [^{11}C]7, and [^{11}C]8

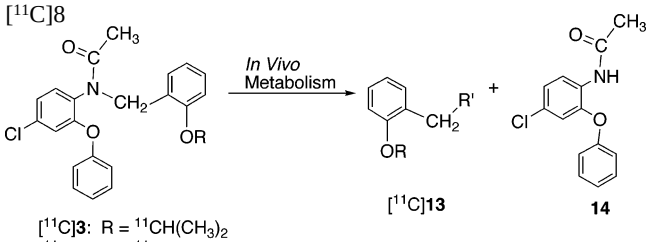

[^{11}C]**3**: R = ^{11}CH(CH$_3$)$_2$
[^{11}C]**7**: R = ^{11}CH$_2$CH$_3$
[^{11}C]**8**: R = ^{11}CH$_3$

most (>95%) of [^{11}C]**7** or [^{11}C]**8** and about 85% of [^{11}C]**3** were detected in the brain homogenate without significant [^{11}C]-metabolites. On the other hand, in the monkey plasma, [^{11}C]-ligands were metabolized with $t_{1/2}$ of 13 min for [^{11}C]**3**, 20 min for [^{11}C]**7**, and 21 min for [^{11}C]**8** (Supporting Information).

As reported previously, debenzylation of **3** was the main route of in vivo metabolism.[27,29,32] Since the ethyl ([^{11}C]**7**) and methyl ([^{11}C]**8**) homologues had molecular similarity to and the bioisoteric property of [^{11}C]**3**, these [^{11}C]ligands may be metabolized by debenzylation to [^{11}C]**13** and **14** with a similar profile (Scheme 3). Since no or a low amount of [^{11}C]**13** with a benzyl moiety was detected in the brain homogenates, its chemical structure was not further identified, although [^{11}C]**13** was extensively determined in the plasma. On the other hand, the debenzylated compound **14**, the main nonradioactive metabolite of the [^{11}C]ligands, had no affinity for PBR (IC_{50} > 10 μM).[27] Therefore, **14** could not interfere with the specific binding of the [^{11}C]ligands to PBR in the brain, even if it passed the BBB and entered the brain. These findings suggested that although the [^{11}C]ligands were rapidly metabolized in the plasma, the specific binding to PBR in the brain was mainly due to these [^{11}C]ligands themselves and was not influenced by their radioactive or nonradioactive metabolites.

Conclusion

In this study, we developed a PBR agonist [^{11}C]**3** and its ethyl ([^{11}C]**7**) and methyl ([^{11}C]**8**) homologues as PET ligands for imaging PBR in the brain. These phenoxyphenyl acetamide derivatives displayed similar affinities for PBR with **2** and higher affinity than **1**. The ^{11}C-labeled ligands were synthesized by alkylation of phenol precursor **9** with [^{11}C]**10**−**12** in reproducible radiochemical yields and relatively high specific activity, respectively. [^{11}C]**3**, [^{11}C]**7**, and [^{11}C]**8** were preferably distributed in the olfactory bulb and cerebellum in the rat brain, consistent with the distribution pattern of PBR. The radioactivity levels of the [^{11}C]ligands in the occipital cortex in the monkey brain were similar to that of [^{11}C]**2** and 3.5−4 times higher than that of [^{11}C]**1**, the standard PET ligand for PBR. Pretreatment experiments revealed that the [^{11}C]**8** binding was inhibited by the PBR-selective **1** or **2**, suggesting that the binding was specific to PBR in the monkey brain. No significant radioactive metabolites of the [^{11}C]ligands were detected in the brain, although they were metabolized by debenzylation in the plasma.

The three alkyl homologues [^{11}C]**3**, [^{11}C]**7**, and [^{11}C]**8** may therefore be promising PET ligands with different properties from the clinically used [^{11}C]**1** and [^{11}C]**2** for investigating PBR in primates. Although their specific binding in the brain was relatively lower, the findings of the in vivo structure−activity relationship are helpful to develop a more favorable PET tracer with improved properties over these ligands.

Experimental Section

^{1}H NMR spectra were recorded on a JNM-GX-270 spectrometer (JEOL, Tokyo) with tetramethylsilane as an internal standard. All chemical shifts (δ) were reported in parts per million (ppm) downfield from the standard. FAB-MS was obtained on a JEOL NMS-SX102 spectrometer (JEOL, Tokyo). Column chromatography was performed using Merck Kieselgel gel 60 F_{254} (70−230 mesh). A CYPRIS HM-18 cyclotron (Sumitomo Heavy Industry, Tokyo) was used for the ^{11}C production by the ^{14}N(p, α)^{11}C nuclear reaction. The purification and analysis of radioactive mixtures was performed by high-performance liquid chromatography (HPLC) with an in-line UV (254 nm) detector in series with a NaI crystal radioactivity detector. Isolated radiochemical yields were determined with an IGC-3 Curiemeter (Aloka, Tokyo). Samples **2**, **3**, and **9** were kindly provided by Dr A. Nakazoto (Taisho Pharmaceutical, Saitama, Japan). All chemical reagents with the highest grade commercially available were purchased from Aldrich Chem. (Milwaukee, WI) and Wako Pure Chem. Ind. (Osaka). All animal experiments were carried out according to the recommendations of the committee for the care and use of laboratory animals, National Institute of Radiological Sciences (NIRS).

***N*-(4-Chloro-2-phenoxyphenyl)-*N*-(2-ethoxylbenzyl)acetamide (7).** A suspension of **9**[25] (38 mg, 0.1 mmol), **11** (16 μL, 0.2 mmol), and NaH (10 mg, 60% in mineral oil, 0.2 mmol) in DMF (4 mL) was stirred at 25 °C for 5 h. The mixture was quenched with AcOEt and washed with water and a saturated NaCl solution. After the organic layer was dried over Na_2SO_4, the solvent was removed to give a residue. Column chromatography of the residue on silica gel with $CHCl_3$/hexane (1/10) gave **7** (34 mg, 86%) as a white powder. Mp: 100−102 °C (103.5−104.0 °C).[25] ^{1}H NMR (300 MHz, $CDCl_3$) δ: 7.10−7.39 (2H, m), 6.28−7.15 (10H, m), 4.68 (2H, dd, $J = 2$, 12 Hz), 4.41 (2H, q, $J = 6$, 8 Hz), 2.12 (3H, s), 1.22 (3H, t, $J = 6$ Hz). FABMS (m/z): 396.1 ($M^+ + 1$). Anal. ($C_{23}H_{22}ClNO_3$) C, H, N.

***N*-(4-Chloro-2-phenoxyphenyl)-*N*-(2-methoxylbenzyl)acetamide (8).** A suspension of **9** (38 mg, 0.1 mmol), **12** (13 μL, 0.2 mmol), and NaH (10 mg, 60% in mineral oil, 0.2 mmol) in DMF (5 mL) was stirred at 25 °C for 3 h. The reaction mixture was treated in a manner similar to that for **7** to obtain **8** (24 mg, 62%) as a white powder. Mp: 109−111 °C (113.0−114.5 °C).[25] ^{1}H NMR (300 MHz, $CDCl_3$) δ: 7.16−7.54 (2H, m), 6.22−7.19 (10H, m), 4.63 (2H, dd, $J = 2$, 12 Hz), 3.80 (3H, s), 2.15 (3H, s). FABMS (m/z): 382.2 ($M^+ + 1$). Anal. ($C_{22}H_{20}ClNO_3$) C, H, N.

***N*-(4-Chloro-2-phenoxyphenyl)-*N*-(2-[2-^{11}C]isopropoxylbenzyl)acetamide ([^{11}C]3).** No-carrier-added [^{11}C]CO_2 (about 37 GBq) was produced by the ^{14}N(p, α)^{11}C nuclear reaction on dry N_2 gas (1.5 Mpa) containing 0.01% O_2 gas with a beam (15 μA) of 18.5 MeV protons (14.2 MeV on 15 cm target) from the cyclotron. During the production of [^{11}C]CO_2, a polyethylene loop for the Grignard reaction was flushed with N_2 and cooled to between −5−0 °C with a liquid N_2 spray. Then, CH_3MgBr solution (1.0 M in THF,

1.0 mL) was loaded into the polypropylene loop. The loop was again flushed with N_2 (2 mL/min) for 30 s to remove excess CH_3MgBr and THF to immobilize a small residue of CH_3MgBr on the inner surface of the loop.

After irradiation, [^{11}C]CO_2 was recovered from the gas target with N_2 (500 mL/min) and concentrated in a stainless steel coil cooled to −150 °C with a liquid N_2 spray until the radioactivity in the coil reached a plateau. On warming, the concentrated [^{11}C]-CO_2 was released and flowed into the loop loaded with CH_3MgBr at −5 °C with dry N_2 (2 mL/min). When the transfer of radioactivity was complete, the N_2 flow was stopped and this loop was then maintained for 5 min at 25 °C for the Grignard reaction. Then, a solution of $LiAH_4$ in THF (0.2 M, 500 μL) was passed through the loop to transfer the reaction mixture into a heated reactor for 1 min at 180 °C. After cooling the reactor to 50−60 °C, aqueous HI (57%, 800 μL) was added into this reactor. The reaction mixture was heated to 180 °C, and the formed radioactive fraction was swept by N_2 (50 mL/min) and introduced into the inlet of the Porapak column at ambient temperature. The N_2 flow continued for 3 min until the radioactivity level plateaued in the column inlet. On heating this column (rate, 15 °C/30 s), [^{11}C]**10** flowed from the column outlet at 6.0 min and was collected in a receiving vial containing anhydrous DMF (1 mL). At the end of synthesis (EOS), [^{11}C]**10** (3.7−4.4 GBq, $n = 3$) was obtained with a radiochemical purity of >95%.

A suspension of **9** (1.0 mg), [^{11}C]**10** (3.0−3.2 GBq), and NaH (7 μL, 0.5 g/20 mL DMF) in DMF (1 mL) was heated at 130 °C and maintained for 10 min. The reaction mixture containing [^{11}C]-**3** was quenched by the addition of CH_3CN/H_2O (90/10, 0.5 mL) and then applied to a semipreparative column (10 mm i.d. × 250 mm, CAPCELL PAK C_{18}, SHISEIDO) set to the JASCO HPLC system. The column was eluted with CH_3CN/H_2O at a flow rate of 5.0 mL/min, and the desired fraction ($t_R = 8.8$ min) was collected in a flask. After evaporation of the solvents from the flask under reduced pressure at 90 °C, the residue was taken up in 10 mL of sterile saline. A saline solution of [^{11}C]**3** was passed through a sterile 0.22 μm filter into a sterile, pyrogen-free bottle. At EOS, [^{11}C]**3** (180−310 MBq, $n = 3$) was obtained with a radiochemical purity of >98%.

***N*-(4-Chloro-2-phenoxyphenyl)-*N*-(2-[2-^{11}C]ethoxylbenzyl)acetamide ([^{11}C]7).** [^{11}C]**11** was prepared in a manner similar to that for [^{11}C]**10** by performing the reaction of CH_3MgBr with [^{11}C]-CO_2 at −5 °C for 1.5 min. At 4.8 min, [^{11}C]**11** flowed from the gas chromatography column and was collected into a receiving vial containing DMF (1 mL). At EOS, [^{11}C]**11** (3.9−5.3 GBq, $n = 3$) was obtained with a radiochemical purity of >95%.

A suspension of **9** (1.0 mg), [^{11}C]**11** (3.0−3.2 GBq), and NaH (7 μL, 0.5 g/20 mL DMF) in DMF (1 mL) was heated at 50 °C and maintained for 5 min. The reaction mixture was purified using the same column but with CH_3CN/H_2O (80/20), and the desired radioactive fraction ($t_R = 8.1$ min) was obtained. After treatment in a manner similar to that for [^{11}C]**3**, [^{11}C]**7** (300−350 MBq, $n = 3$) was obtained with a radiochemical purity of >98% at EOS.

***N*-(4-Chloro-2-phenoxyphenyl)-*N*-(2-[^{11}C]methoxylbenzyl)acetamide ([^{11}C]8).** The preparation of [^{11}C]**12** and subsequent [^{11}C]-methylation of **9** to [^{11}C]**8** were achieved automatically using specially designed equipment.[38] Briefly, the cyclotron-produced [^{11}C]CO_2 (about 10 GBq) was bubbled into a reactor containing a solution of $LiAlH_4$ in THF (0.2 M, 500 μL). Upon evaporation of the THF at 180 °C, 57% aqueous HI (300 μL) was added to the reactor. The formed [^{11}C]**12** was distilled, passed through an Ascarite and P_2O_5 column, and collected in a vessel containing **9** (1.0 mg), NaH (7 μL, 0.5 g/20 mL DMF), and DMF (1 mL) for 1.5 min at −15 to −20 °C. The reaction vessel was then heated to 30 °C and maintained for 5 min. The reaction mixture was purified by the same column but with CH_3CN/H_2O (70/30), and the desired radioactive fraction ($t_R = 9.5$ min) was collected. After treatment in a manner similar to that for [^{11}C]**3**, [^{11}C]**8** (1.0−1.3 GBq, $n = 3$)was obtained with a radiochemical purity of >98% at EOS.

Radiochemical Purity and Specific Activity Determinations. Aliquots of the formulated solutions were used to establish the chemical and radiochemical purity and specific activity employing analytical HPLC (column, CAPCELL PAK C_{18}, 4.6 mm i.d. × 250 mm; UV at 254 nm; mobile phase, $CH_3CN/H_2O = 6/4$). The t_R values for [^{11}C]**3**, [^{11}C]**7**, and [^{11}C]**8** were 9.8, 6.5, and 6.0 min at a flow rate of 2.0 mL/min, respectively. The specific activity of these products was determined by comparing the assayed radioactivity to the mass measured from the carrier UV peak at 254 nm.

Octanol−Water Partition Coefficient. [^{11}C]**3**, [^{11}C]**7**, or [^{11}C]-**8** (3−5 MBq/0.2 mL) was added to a mixture of 1-octanol (5 mL) and 10 mM phosphate buffer (pH 7.4, 5 mL), shaken vigorously, and allowed to equilibrate for 1 h at room temperature. The ^{11}C concentrations in the organic and aqueous phases were measured using an autogamma counter, and each partition coefficient was calculated as the ratio of the concentration in the organic phase to that in the aqueous phase.[40]

In Vitro Binding Assays. Male Sprague−Dawley rats ($n = 4$) weighing 220−250 g were killed by decapitation under ether anesthesia, and their brains were quickly removed and frozen on powdered dry ice. Brain sagittal sections (20 μm) were cut on a cryostat microtome (HM560, Carl Zeiss, Germany) and thaw-mounted on glass slides (Matsunami Glass Ind., Tokyo), which were then dried at room temperature and stored at −18 °C until used for experiments. The brain sections were preincubated at 25 °C for 20 min in 50 mM Tris-HCl (pH 7.4) buffer. After preincubation, these sections were incubated at 37 °C for 30 min in the assay buffer containing [^{11}C]**2** (1 nM; specific activity, 110 GBq/μmol) or [^{11}C]-flumazenil (1 nM; specific activity, 210 GBq/μmol). To determine the IC_{50} values of **1**−**3**, **7**, and **8** for the [^{11}C]**2** (PBR) or [^{11}C]-flumazenil (CBR) binding, brain sections were incubated with [^{11}C]-**2** or [^{11}C]flumazenil in the presence of increasing concentrations of the corresponding **1**−**3**, **7**, and **8** (0.1−1000 nM). Nonradioactive **2** and flumazenil (1 μM) were used to determine the nonspecific bindings for PBR and CBR, respectively. After incubation, the sections were washed three times for 2 min each time with the cold assay buffer, dipped in cold distilled water, and dried with warm air. These sections were then placed in contact with imaging plates (BAS−SR 127, Fuji Photo Film, Tokyo) for 60 min to analyze the distribution of their radioactivities with a FUJIX BAS 1800II bioimaging analyzer (Fuji). The region of interest (ROI) of the sections was placed on the cerebellum and the radioactivity in the ROI was expressed as photostimulated luminescence (PSL) values. PSL data corresponding to the radioactivity of the cerebellum in the presence and absence of the displaced **1**−**3**, **7**, and 8 were determined. Specific binding for PBR or CBR was defined as total binding minus binding in the presence of **2** or flumazenil (1 μM). The PSL data corresponding to the specific binding at each compound concentration were calculated as the percentages in relation to the control specific bindings, which were converted to probit values to determine the IC_{50} of each compound. The IC_{50} value was further converted to K_i according to the Cheng−Prusoff equation.

Ex Vivo Autoradiography. A saline solution of [^{11}C]**3**, [^{11}C]**7**, or [^{11}C]**8** (45−50 MBq/200 μL) was injected into a male Sprague−Dawley rat (220−250 g, 9 weeks, SLC, Shizuoka, Japan; $n = 3$/[^{11}C]ligand) through the tail vein. At 30 min after injection, the rat was sacrificed by decapitation under ether anesthesia, and the brain was quickly removed and frozen on powdered dry ice. Brain sagittal sections (20 μm) were cut on a cryostat microtome (HM560), thaw-mounted on glass slides, and dried with warm air. These sections were then placed in contact with imaging plates (BAS−SR 127) for 60 min to analyze the radioactivity distribution with the bioimaging analyzer.

For the inhibition experiments, a mixture of [^{11}C]**3**, [^{11}C]**7**, or [^{11}C]**8** (45−50 MBq/200 μL) and **2** (1 mg/kg, 10% EtOH in 200 μL saline) was used as described above.

Monkey PET. PET scan was performed using a high-resolution SHR-7700 PET camera (Hamamatsu Photonics, Hamamatsu, Japan) designed for laboratory animals that provides 31 transaxial slices 3.6 mm (center-to-center) apart and a 33.1 cm field of view. The same awake rhesus monkey (*Macaca mulatta*, male, SLC, Shizuoka, Japan) weighing about 7.5 kg was used for all PET scans.

Afterward, transmission scans for attenuation correction were performed for 1 h using a 74 MBq $^{68}Ge-^{68}Ga$ source. A dynamic emission scan in the 3D acquisition mode was performed for 90 min (1 min × 4 frames, 2 min × 8 frames, 5 min × 8 frames, 10 min × 3 frames). All emission scan images were reconstructed with a Colsher filter of 4 mm, and circular regions of interest (ROIs) with a 5-mm diameter were placed over the occipital cortex using image analysis software.[30] A solution of [^{11}C]**3**, [^{11}C]**7**, or [^{11}C]**8** (70−80 MBq/2 mL) was injected iv into the monkey, and time-sequential tomographic scanning was performed on a transverse section of the brain for 90 min. In pretreatment experiments, nonradioactive **2** (1 mg/kg, 10% EtOH in 1 mL saline) or **1** (5 mg/kg, 10% EtOH in 2 mL saline) was injected 2 min before the [^{11}C]ligand injection. The time−activity curves in the occipital cortex were obtained for each scan of the brain.

Metabolite Analysis for Mouse Plasma and Brain Homogenate. Three mice (ddy, male, SLC; Shizuoka, Japan) were injected with [^{11}C]**3**, [^{11}C]**7**, or [^{11}C]**8** (30−40 MBq/200 μL) via the tail vein. After the mice were sacrificed by cervical dislocation at 1, 5, 15, 30, or 60 min, blood (0.5−1.0 mL) was collected from the heart, and the whole brain was surgically removed from the skull and stored on ice. The blood sample was centrifuged at 15 000 rpm for 1 min at 4 °C to separate plasma, of which 250 μL was collected in a test tube containing CH_3CN (500 μL) and a solution of the authentic nonradioactive **3**, **7**, or **8** (1.0−1.5 mg/5.0 mL CH_3CN, 10 μL). After the tube was vortexed for 15 s and centrifuged at 15 000 rpm for 2 min for deproteinization, the supernatant was collected. The extraction efficiency of radioactivity into the CH_3CN supernatant ranged from 84% to 92% of the total radioactivity in the plasma. On the other hand, the cerebellum and forebrain, including the olfactory bulb, were dissected from the mouse brain and homogenized together in an ice-cooled CH_3CN/H_2O (1/1, 1.0 mL) solution. The homogenate was centrifuged at 15 000 rpm for 1 min at 4 °C and the supernatant was collected. The recovery of radioactivity into the supernatant was 70−91% based on the total radioactivity in the brain homogenate.

An aliquot of the supernatant (100−500 μL) obtained from the plasma or brain homogenate was injected into the HPLC system for radioactivity and analyzed under the same conditions described. The percent ratio of the [^{11}C]ligand to total radioactivity (corrected for decay) on the HPLC chromatogram was calculated as % = (peak area for [^{11}C]ligand/total peak area) × 100.

Metabolite Analysis for Monkey Plasma. After iv injection of [^{11}C]**3**, [^{11}C]**7**, or [^{11}C]**8** (70−80 MBq) into the monkey, arterial blood samples (1 mL) were collected at 1, 2, 5, 10, 20, 30, and 60 min. All samples were centrifuged at 15 000 rpm for 1 min at 4 °C to separate plasma, of which 250 μL was collected in a test tube containing CH_3CN (0.5 mL). The tube was vortexed for 15 s and centrifuged at 15 000 rpm for 1 min for deproteinization. The extraction efficiency of radioactivity into the CH_3CN ranged from 73% to 94% of the total radioactivity in the plasma. The radioactive fractions in these samples were analyzed using HPLC.

Acknowledgment. The authors are grateful to Taisho Pharmaceutical Co., Ltd. (Saitama, Japan) for providing samples (**2**, **3**, and **9**). We also thank the crew of the Cyclotron Operation Section and Radiopharmaceutical Chemistry Section of National Institute of Radiological Sciences (NIRS) for support in operation of the cyclotron and production of radioisotopes.

Supporting Information Available: Percent conversion of [^{11}C]-**3**, [^{11}C]**7**, or [^{11}C]**8** to metabolite in the monkey plasma at several time points after iv injection of the [^{11}C]ligand (70−80 MBq) into the monkey, where all results were presented as mean values (n = 3) with a maximum range of ± 5%; results of elemental analysis; and HPLC chromatograms. This material is available free of charge via the Internet at http://pubs.acs.org.

References

(1) Doble, A.; Ferris, O.; Burgevin, M. C.; Menager, J.; Uzan, A.; Dubroeucq, M. C.; Renault, C.; Gueremy, C.; Le Fur, G. Photoaffinity Labeling of Peripheral-type Benzodiazepine Binding Sites. *Mol. Pharmacol.* **1987**, *31*, 42−49.

(2) Anholt, R. R.; Pedersen, P. L.; DeSouza, E. B.; Snyder, S. H. The Peripheral-type Benzodiazepine Receptor: Localization to the Mitochondrial Outer Membrane. *J. Biol. Chem.* **1986**, *261*, 576−583.

(3) Culty, M.; Li, H.; Boujrad, N.; Bernassau, J. M.; Reversat, J. L.; Amri, H.; Vidic, B.; Papadopoulos, V. In Vitro Studies on the Role of the Peripheral Benzodiazepine Receptor in Steroidogenesis. *J. Steroid Biochem. Mol. Biol.* **1999**, *69*, 123−130.

(4) Braestrup, C.; Squires, R. F. Specific Benzodiazepine Receptors in Rat Brain Characterized by High Affinity [^{3}H]Dizaepam Binding. *Proc. Natl. Acad. Sci. U.S.A.* **1977**, *74*, 3805−3809.

(5) Anholt, R. R.; De Souza, E. B.; Oster-Granite, M. L.; Synder, S. H. Peripheral-type Benzodiazepine Receptors: Autoradiographic Localization in Whole-body Sections of Neonatal Rats. *J. Pharmacol. Exp. Ther.* **1985**, *233*, 517−526.

(6) Gavish, M.; Katz, Y.; Bar-Ami, S.; Weizman, R. Biochemical, Physiological and Pathological Aspects of the Peripheral Benzodiazepine Receptor. *J. Neurochem.* **1992**, *58*, 1589−1601.

(7) Benavides, J.; Guilloux, F.; Rufat, P.; Uzan, A.; Renault, C.; Dubroeucq, M. C.; Gueremy, C.; Le Fur, G. In Vivo Labeling in Several Rat Tissues of 'Peripheral Type' Benzodiazepine Binding Sites. *Eur. J. Pharmacol.* **1984**, *99*, 1−7.

(8) Benavides, J.; Quarteronet, D.; Imbault, F.; Malgouris, C.; Uzan, A.; Renault, C.; Dubroeucq, M. C.; Gueremy, C.; Le Fur, G. Labeling of 'Peripheral-type' Benzodiazepine Binding Sites in the Rat Brain by Using [3H]PK 11195, an Isoquinoline Carboxamide Derivative: Kinetic Studies and Autoradiographic Localization. *J. Neurochem.* **1983**, *41*, 1744−1750.

(9) Zisterer, D. M.; Williams, D. C. Peripheral-type Benzodiazepine Receptors. *Gen. Pharmacol.* **1997**, *29*, 305−314.

(10) Anholt, R. R.; Murphy, K. M.; Mack, G. E.; Snyder, S. H. Peiperal-type Benzodiazepine Receptors in the Central Nervous System: Localization to Olfactory Nervous. *J. Neurosci.* **1984**, *4*, 593−603.

(11) Petit-Taboué, M. C.; Baron, J. C.; Barré, L.; Travère, J. M.; Speckel, D.; Camsonne, R.; MacKenzie, E. T. Brain Kinetics and Specific Binding of [^{11}C]PK 11195 to Omaga3 Sites in Baboons: Positron Emission Tomography Study. *Eur. J. Pharmacol.* **1991**, *200*, 347−351.

(12) Rao, V. L.; Butterworth, R. F. Characterization of Binding Sites for the Omega3 Receptors Ligands [^{3}H]PK11195 and [^{3}H]Ro5-4864 in human brain. *Eur. J. Pharmacol.* **1997**, *340*, 89−90.

(13) Faure, J. P.; Hauet, T.; Han, Z.; Goujon, J. M.; Petit, I.; Mauco, G.; Eugene, M.; Carretier, M.; Papadopoulos, V. Polyethylene Glycol Reduces Early and Long-Term Cold Ischemia−Reperfusion and Renal Medulla Injury. *J. Pharmacol. Exp. Ther.* **2002**, *302*, 861−870.

(14) Versijpt, J. J.; Dumont, F.; Van Laere, K. J.; Decoo, D.; Santens, P.; Audenaert, K.; Achten, E.; Slegers, G.; Dierckx, R. A.; Korf, J. Assessment of Neuroinflammation and Microglial Activation in Alzheimer's Disease with Radiolabelled PK11195 and Single Photon Emission Computed Tomography. A Pilot Study. *Eur. Neurol.* **2003**, *50*, 39−47.

(15) Neary, J. T.; Jorgensen, S. L.; Oracion, A. M.; Bruce, J. H.; Norenberg, M. D. Inhibition of Growth Factor-Induced DNA Synthesis in Astrocytes by Ligands of Peripheral-type Benzodiazepine Receptors. *Brain Res.* **1995**, *675*, 27−30.

(16) Weizman, R.; Gavish, M. Molecular, Cellular and Behavioral Aspects of Peripheral-type Benzodiazepine Receptors. *Clin. Neuropharmacol.* **1993**, *16*, 401−417.

(17) Maaser, K.; Grabowski, P.; Sutter, A. P.; Hopfner, M.; Foss, H. D.; Stein, H.; Berger, G.; Gavish, M.; Zeitz M, Scherubl, H. Overexpression of the Peripheral Benzodiazepine Receptor is a Relevant Prognostic Factor in Stage III Colorectal Cancer. *Clin. Cancer Res.* **2002**, *8*, 3205−3209.

(18) Camsonne, R.; Crouzel, C.; Comar, D.; Maziere, M.; Prenant, C.; Sastre, J.; Moulin, M. A.; Syrota, A. Synthesis of N-[^{11}C]-Methyl, N-(Methyl-1-propyl), (Chloro-2-phenyl)-1-isoquinoline Carboxamide-3 (PK11195): A New Ligand for Peripheral Benzodiazepine Receptors. *J. Labelled Compd. Radiopharm.* **1984**, *21*, 985−991.

(19) Cappelli, A.; Anzini, M.; Vomero, S.; De Benedetti, P. G.; Menziani, M. C.; Giorgi, G.; Manzoni, C. Mapping the Peripheral Benzodiazepine Receptor Binding Site by Conformationally Restrained Derivatives of 1-(2-Chlorophenyl)-1-*N*-methypropyl-3-isoquinolinecarboxamide (PK11195). *J. Med. Chem.* **1997**, *40*, 2910−2921.

(20) Matarrese, M.; Moresco, R. M.; Cappelli, A.; Anzini, M.; Vomero, S.; Simonelli, P.; Verza, E.; Magni, F.; Sudati, F.; Soloviev, D.; Todde, S.; Carpinelli, A.; Kienle, M. G.; Fazio, F. Labeling and Evaluation of *N*-[^{11}C]Methylated Quinoline-2-carboxamides as Potential Radioligands for Visualization of Peripheral Benzodiazepine Receptors. *J. Med. Chem.* **2001**, *44*, 579−585.

(21) Mattner, F.; Katsifis, A.; Staykova, M.; Ballantyne, P.; Willenborg, D. O. Evaluation of a Radiolabelled Peripheral Benzodiazepine Receptor Ligand in the Central Nervous System Inflammation of Experimental Autoimmune Encephalomyelitis: A Possible Probe for Imaging Multiple Sclerosis. *Eur. J. Nucl. Med. Mol. Imaging* **2005**, *32*, 557−563.

(22) Kassiou, M.; Meikle, S. R.; Banati, R. B. Ligands for Peripheral Benzodiazepine Binding Sites in Glial Cells. *Brain Res*. **2005**, *48*, 207−210.

(23) Pappata, S.; Cornu, P.; Samson, Y.; Prenant, C.; Benavides, J.; Scatton, B.; Crouzel, C.; Hauw, J. J.; Syrota, A. PET Study of Carbon-11-PK11195 Binding to Peripheral Type Benzodiazepine Sites in Glioblastoma: A Case report. *J. Nucl. Med.* **1991**, *32*, 1608−1610.

(24) Debruyne, J. C.; Van Laere, K. J.; Versijpt, J.; De Vos, F.; Eng, J. K.; Strijckmans, K.; Santens, P.; Achten, E.; Slegers, G.; Korf, J.; Dierckx, R. A.; De Reuck, J. L. Semiquantification of the Peripheral-type Benzodiazepine Ligand [11C]PK11195 in Normal Human Brain and Application in Multiple Sclerosis Patients. *Acta Neurol. Belg.* **2002**, *102*, 127−135.

(25) Okubo, T.; Yoshikawa, R.; Chaki, S.; Okuyama, S.; Nakazato, A. Design, Synthesis and Structure-affinity Relationships of Aryloxyanilide Derivatives as Novel Peripheral Benzodiazepine Receptor Ligands. *Bioorg. Med. Chem.* **2004**, *12*, 423−438.

(26) Chaki, S.; Funakoshi, T.; Yoshikawa, R.; Okuyama, S.; Okubo, T.; Nakazato, A.; Nagamine, M.; Tomisawa, K. Binding Characteristics of [3H]DAA1106, a Novel and Selective Ligand for Peripheral Benzodiazepine Receptors. *Eur. J. Pharmacol.* **1999**, *371*, 197−204.

(27) Okuyama, S.; Chaki, S.; Yoshikawa, R.; Ogawa, S.; Suzuki, Y.; Okubo, T.; Nakazato, A.; Nagamine, M.; Tomisawa, K. Neuropharmacological Profile of Peripheral Benzodiazepine Receptor Agonists, DAA1097 and DAA1106. *Life Sci.* **1999**, *64*, 1455−1564.

(28) Culty, M.; Silver, P.; Nakazato, A.; Gazouli, M.; Li, H.; Muramatsu, M.; Okuyama, S.; Papadopoulos, V. Peripheral Benzodiazepine Receptor Binding Properties and Effects on Steroid Synthesis of Two New Phenoxy Phenylacetamide Derivatives, DAA1097 and DAA1106. *Drug Dev. Res.* **2001**, *52*, 475−484.

(29) Zhang, M.-R.; Kida, T.; Noguchi, J.; Furutsuka, K.; Maeda, J.; Suhara, T.; Suzuki, K. [^{11}C]DAA1106: Radiosynthesis and In Vivo Binding to Peripheral Benzodiazepine Receptors in Mouse Brain. *Nucl. Med. Biol.* **2003**, *30*, 513−519.

(30) Maeda, J.; Suhara, T.; Zhang, M.-R.; Okauchi, T.; Yasuno, F.; Ikoma, Y.; Inaji, M.; Nagai, Y.; Ichimiya,; Ohbayashi, S.; Suzuki, K. Novel Peripheral Benzodiazepine Receptor Ligand [^{11}C]DAA1106 for PET. An Imaging Tool for Glial Cells in the Brain. *Synapse* **2004**, *52*, 283−291.

(31) Zhang, M.-R.; Maeda, J.; Furutsuka, K.; Yoshida, Y.; Ogawa, M.; Suhara, T.; Suzuki, K. [^{18}F]MDAA1106 and [^{18}F]FEDAA1106: Two Positron-Emitter Labeled Ligands for Peripheral Benzodiazepine Receptor (PBR). *Bioorg. Med. Chem. Lett.* **2003**, *13*, 201−204.

(32) Zhang, M.-R.; Maeda, J.; Ogawa, M.; Noguchi, J.; Ito, T.; Yoshida, Y.; Okauchi, T.; Obayashi, S.; Suhara, T.; Suzuki, K. Devlopment of a New Radioligand, *N*-(5-Fluoro-2-phenoxyphenyl)-*N*-(2-[^{18}F]-fluoroethoxyl-5-methoxybenzyl)acetamide, for PET Imaging of Peripheral Benzodiazepine Receptor in Primate Brain. *J. Med. Chem.* **2004**, *47*, 2228−2235.

(33) Zhang, M.-R.; Maeda, J.; Ito, T.; Okauchi, T.; Ogawa, M.; Noguchi, J.; Suhara, T.; Halldin, C.; Suzuki, K. Synthesis and Evaluation of *N*-(5-Fluoro-2-phenoxyphenyl)-*N*-(2-[^{18}F]fluoromethoxy-d_2-5-methoxybe nzyl)acetamide: A Deuterium-Substituted Radioligand for Peripheral Benzodiazepine Receptor. *Bioorg. Med. Chem.* **2005**, *13*, 1811−1818.

(34) Langstrom, B.; Antoni, G.; Gullberg, P.; Halldin, C.; Nagren, K.; Rimland, A.; Svard, H. 1986. The Synthesis of 1-^{11}C-Labelled Ethyl, Propyl, Butyl and Isobutyl Iodides and Examples of Alkylation Reactions. *Appl. Radiat. Isot.* **1986**, *37*, 1141−1145.

(35) Slegers, G.; Sambre, J.; Goethals, P.; Vandecasteele, C.; Van Haver, D. Synthesis of [1-^{11}C]Iodoethane for the Preparation of [^{11}C]Ethyl Labeled Radiopharmaceuticals. *Appl. Radiat. Isot.* **1986**, *37*, 279−282.

(36) Suzuki, K. Development of a Multi-purpose Equipment of the Repeated Synthesis of ^{11}C-Labeled Alkyl Iodides with High Specific Activity. *Radiochimica Acta* **1990**, *50*, 49−53.

(37) Zhang, M.-R.; Ogawa, M.; Yoshida, Y.; Suzuki, K. Selective Synthesis of [2-^{11}C]Isopropyl Iodide and [1-^{11}C]Ethyl Iodide Using Loop Method by Reaction of Methylmagnesium Bromide with [^{11}C]-Carbon Dioxide. *Appl. Radia. Isot.* **2006**, *64*, 216−222.

(38) Suzuki, K.; Inoue, O.; Hashimoto, K.; Yamasaki, T.; Kuchiki, M.; Tamate, K. Computer-Controlled Large Scale Production of High Specific Activity [^{11}C]Ro15-1788. *Appl. Radiat. Isot.* **1985**, *36*, 971−976.

(39) Hashimoto, K.; Inoue, O.; Suzuki, K.; Yamasaki, T.; Kojima, M. Synthesis and Evaluation of ^{11}C-PK11195 for In Vivo Study of Peripheral-type Benzodiazepine Receptors Using Positron Emission Tomography. *Ann. Nucl. Med.* **1989**, *3*, 63−71.

(40) Zhang, M.-R.; Kikuchi, T.; Yoshida, Y.; Maeda, J.; Kida, T.; Okauchi, T.; Irie, T.; Suzuki, K. *N*-[^{18}F]Fluoroethyl-4-piperidyl Acetate ([^{18}F]-FEtP4A): A PET Tracer for Imaging Brain Acetylcholinesterase In Vivo. *Bioorg. Med. Chem.* **2003**, *11*, 2519−2527.

JM060006K